ROD AND CONE CONTRIBUTIONS TO MESOPIC VISION

Joel Pokorny [1] and Dingcai Cao [2]

[1]Visual Science Laboratories, University of Chicago, USA

[2] Dept. of Surgery, Section of Ophthalmology and Visual Science, University of Chicago, USA

ABSTRACT

Mesopic light levels span approximately 3-4 log units in the natural viewing environment, including many indoor lighting settings, and most twilight or nighttime outdoor and traffic lighting environments. Traditional studies of the contribution of the different photoreceptor types to mesopic vision have been hampered by an inability to modulate the rod or cone systems independently. Our approach differs from the traditional studies in employing a four-primary method that allows independent control of the stimulation of the four receptor types in a stimulus field. We developed a general method for adjusting the radiances of four lights to silence up to three photoreceptor classes and change the excitation of the nonsilenced classes in a specified manner. Here, we include an overview of rod anatomy and physiology and a description of the logic and implementation of the four-primary methodology. Data and analysis are given for two functional areas that may impact lighting solutions; dark-adapted rods suppress cone vision, and how rod and cone reaction times vary at scotopic, mesopic and photopic adaptation levels.

Keywords: rods, cones, mesopic vision, four-primary method, rod pathways

1. INTRODUCTION

There is a literature on the effects on visual performance of illuminants differing in spectral composition under photopic, mesopic and scotopic conditions (He *et al.*, 1997; Rea *et al.*, 1997; Adrian, 1998; Lewis, 1999; Walkey *et al.*, 2007). For lights equated for photopic function, performance at mesopic and scotopic levels degrades most for illuminants deficient in short wavelength light. Here, we present two sets of experiments that show the scientific basis for the reported empirical results. The experiments use a four-primary photostimulator we devised, which allows independent control of the stimulation of the four photoreceptor types in the human retina. We developed a general method for adjusting the radiances of the four lights to silence up to three photoreceptor classes and change the excitation of the nonsilenced class in a specified manner. We provide examples from two studies related to mesopic temporal processing. The first investigates the suppression of cone flicker detection by dark adapted rods. The second provides systematic reaction time measurements for stimuli that isolated rod and cone excitation at light levels ranging from scotopic to photopic.

In this article, we review anatomical and physiological studies related to mesopic vision, the theoretical and technical aspects of the four-primary methodology, and some unique findings concerning mesopic temporal processing.

2. RODS AND CONES SHARE NEURAL PATHWAYS FROM EYE TO BRAIN

Modern anatomical and physiological studies have identified three major neural retinogeniculate pathways in the primate visual system that convey retinal information into visual cortex (reviewed by Dacey, 2000). The pathways are named after the layers of lateral geniculate nucleus (LGN) that receive inputs from distinct types of ganglion cells and project to different areas of primary visual cortex. The Magnocellular layer of LGN receives inputs from parasol ganglion cells. This pathway (the so-called Magnocellular, MC-pathway) processes the summed output of the long (L-) and middle (M-) wavelength sensitive cones to signal luminance information. Both cone types contribute to the center and surround of the receptive field of MC-cells (Lee, 1996). The Parvocellular layer of the LGN receives inputs from midget ganglion cells. This pathway (so-called Parvocellular, PC-pathway) mediates spectral opponency of L- and M- cones to signal chromatic and luminance information. PC-ganglion cells have the classical center-surround receptive field configuration. Four subgroups of PC-cells have been identified: +L/-M ("Red-ON"), -L/+M ("Red-OFF"), +M/-L ("Green-ON") and –M/+L ("Green-OFF") cells. Each cell type shows the characteristic response of center and surround receptive fields for

cone contrast. The Koniocellular (KC-) layer of LGN receives inputs from small bistratified as well as other ganglion cells (Dacey & Lee, 1994). This pathway (so-called the Koniocellular, KC- pathway) differences short wavelength (S-) cone signals from the sum of the L- and M- cones.

The link between the three retinogeniculate pathways to psychophysics is well established. Physiological recordings (Derrington *et al.*, 1984; Lee *et al.*, 1990) indicate that MC-, PC- and KC- cells show preferred response to luminance (L+M), chromatic [L/(L+M)], and S/(L+M) signals, respectively. Therefore, psychophysical experiments can be designed to *infer* the functions of the MC-, PC-, and KC-pathways by varying (L+M), L/(L+M), and S/(L+M), respectively (Pokorny & Smith, 2004).

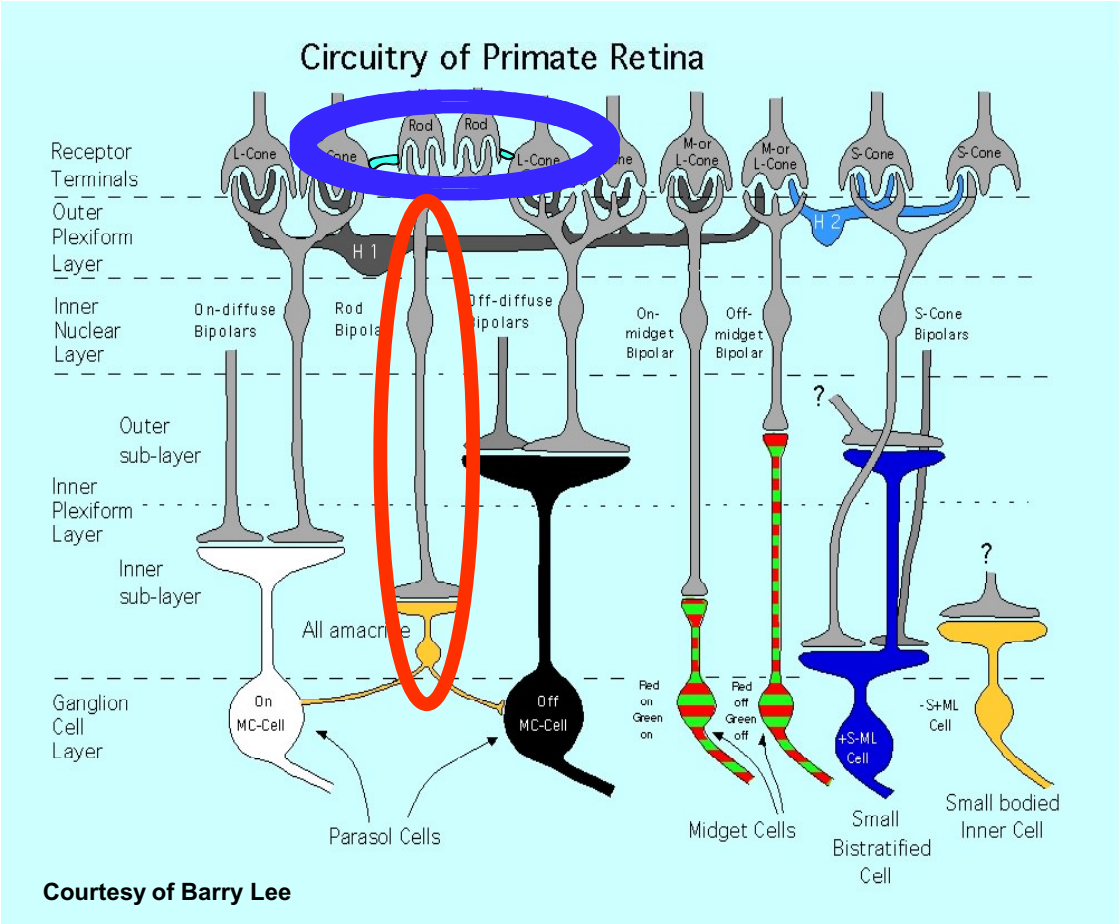

Figure 1. Rod pathways in the primate retina. Slow pathway: Rods->Rod Bipolars->AII Amacrine Cells->Cone Bipolars (red ellipse); Fast pathway: Rods->Cones->Cone Bipolars (blue ellipse).

Anatomical and single-unit electrophysiological studies have shown that rods and cones share neural pathways and have joint inputs to retinal ganglion cells (reviewed by Daw *et al.*, 1990; Sharpe & Stockman, 1999). Rod signals are conveyed to ganglion cells by two primary pathways whose contributions are dependent on the illumination level. One pathway is via ON rod bipolars, AII amacrine cells, and ON and OFF cone bipolars. This is a slow but high gain pathway and is hypothesized to mediate rod vision at low light levels. The second pathway transmits rod information via rod–cone gap junctions and ON and OFF cone bipolars. This is a fast pathway and is hypothesized to mediate rod vision at high scotopic and mesopic light levels (Figure 1). A third insensitive rod pathway between rods and OFF cone bipolars has been identified, but so far has been evident only in rodents.

Several physiological studies have assessed rod input to the three major retinogeniculate pathways. A consistent finding is that there is strong rod input to the MC- pathway, either at the ganglion cell

level (Gouras & Link, 1966; Virsu & Lee, 1983; Virsu *et al.*, 1987; Lee *et al.*, 1997) or the LGN level (Purpura *et al.*, 1988). The demonstration of rod input to the PC- and KC-pathways is less clear. Some studies have shown weak rod input to the PC-pathway (Wiesel & Hubel, 1966; Virsu *et al.*, 1987; Lee *et al.*, 1997) and at least one study did not find any measurable rod input (Purpura et al., 1988). Lee et al. (1997) found no rod input to parafoveal +S/-(L+M) ganglion cells, but two recent studies have demonstrated strong rod input in the retinal periphery (Crook *et al.*, 2009; Field *et al.*, 2009).

3. LIMITATIONS OF CONVENTIONAL METHODOLOGIES FOR STUDYING MESOPIC VISION

Traditional studies of the contribution of the different photoreceptor types to mesopic vision have been limited by an inability to modulate one or the other of the receptor systems independently. There are three traditional strategies in observers with normal vision and each has shortcomings. The first takes advantage of the fact that rods and cones recover sensitivity in the dark at different rates following the termination of a desensitizing light. The increase in visual sensitivity in the dark has two phases. During the first phase, cones mediate thresholds, and visual sensitivity increases rapidly before stabilizing within 10 minutes. The time period in which cone-mediated sensitivity remains stable is called the cone plateau. During the second phase, rods mediate thresholds and sensitivity increases gradually, stabilization occurs following 20-30 minutes. Measurements obtained under dark-adapted and cone-plateau conditions have been compared to characterize potential rod contributions (e.g. Stabell & Stabell, 1999). This approach has the limitation that the two measurements are made under differing adaptation conditions, and visual function depends on adaptation. A second traditional strategy is to compare measurements obtained from foveal and parafoveal presentations (e.g. Thomas & Buck, 2006). The rationale is that the density of rods is high in the peripheral retina but there are few or no rods in the fovea. Evidence has shown, however, that the temporal properties of rod vision and the chromatic properties of cone vision vary with retinal location, which may make comparisons between data collected in the fovea and parafovea ambiguous. A third strategy is use one chromaticity to favor rod isolation and another chromaticity to favor cone isolation (e. g. Conner, 1982; Frumkes *et al.*, 1986). This strategy has a drawback; measurements are limited to light levels where rods are more sensitive than cones. This strategy cannot completely isolate rod activity because, in the dark adapted eye, rods and cones have roughly the same sensitivity at long wavelengths (Crawford & Palmer, 1985) and S- and M- cones do not completely adapt to a long wavelength light. Further, there is a chromatic component to the cone stimulus that may alter measured function.

4. FOUR-PRIMARY COLORIMETRY: METHOD FOR INDEPENDENTLY STIMULATING RODS AND CONES AT A COMMON ADAPTATION LEVEL

4.1. Theoretical basis

There are four types of photoreceptors in human retina, including short-wavelength sensitive cones (S-cones), middle-wavelength sensitive cones (M-cones), long-wavelength sensitive cones (L-cones) and rods. The theoretical basis for achieving independent control of the activities of four types of photoreceptors (S-cones, M-cones, L-cones and rods) in the human retina is silent substitution (Estévez & Spekreijse, 1982) and the details are provided by Shapiro et al (1996). In short, the rod spectral sensitivity, $\bar{r}(\lambda)$, is characterized by the CIE scotopic luminosity function, $V'(\lambda)$, and the S, M and L cone spectral sensitivities, $\bar{s}(\lambda)$, $\bar{m}(\lambda)$, and $\bar{l}(\lambda)$, by the Smith-Pokorny cone fundamentals (Smith & Pokorny, 1975) applied to the CIE 1964 10° color matching functions (Shapiro et al., 1996). The relative spectral sensitivity functions of the S-, M-, L-cones and the rods are shown in Figure 2.

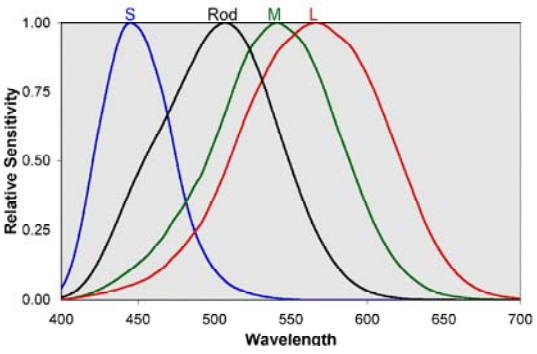

Figure 2.The spectral sensitivity functions of the S-, M-, L- cones and rods.

For any light source with the spectral distribution of $\tilde{Q}(\lambda)$, the S, M, L cone excitations and rod excitations (R) are computed as:

$$S = C_{p,K_m} \sum_{\lambda} \tilde{Q}(\lambda)\bar{s}(\lambda) \quad (1)$$

$$M = C_{p,K_m} \sum_{\lambda} \tilde{Q}(\lambda)\bar{m}(\lambda) \quad (2)$$

$$L = C_{p,K_m} \sum_{\lambda} \tilde{Q}(\lambda)\bar{l}(\lambda) \quad (3)$$

$$R = C_{p,K_m} \sum_{\lambda} \tilde{Q}(\lambda)\bar{r}(\lambda) \quad (4)$$

where $C_{p,Km}$ is a factor equal to the pupil size times K_m, a constant that relates lumens to watts. For a four-primary photostimulator, suppose that the spectral distributions of the four LEDs at their maximal outputs are $\tilde{P}_{1,\lambda}$, $\tilde{P}_{2,\lambda}$, $\tilde{P}_{3,\lambda}$, $\tilde{P}_{4,\lambda}$. With α= [p_1 p_2 p_3 p_4] representing the proportion of its maximum for each LED, the photoreceptor excitations β= [*S M L R*] can be computed using linear algebra $\beta=\alpha A$, where *A* is a matrix with each row representing photoreceptor excitations at the maximum output of each LED (see Equation 5).

$$\mathbf{A} = C_{p,K_m}\begin{bmatrix} \sum_{\lambda}\tilde{P}_{1,\lambda}\bar{s}(\lambda) & \sum_{\lambda}\tilde{P}_{1,\lambda}\bar{m}(\lambda) & \sum_{\lambda}\tilde{P}_{1,\lambda}\bar{l}(\lambda) & \sum_{\lambda}\tilde{P}_{1,\lambda}\bar{r}(\lambda) \\ \sum_{\lambda}\tilde{P}_{2,\lambda}\bar{s}(\lambda) & \sum_{\lambda}\tilde{P}_{2,\lambda}\bar{m}(\lambda) & \sum_{\lambda}\tilde{P}_{2,\lambda}\bar{l}(\lambda) & \sum_{\lambda}\tilde{P}_{2,\lambda}\bar{r}(\lambda) \\ \sum_{\lambda}\tilde{P}_{3,\lambda}\bar{s}(\lambda) & \sum_{\lambda}\tilde{P}_{3,\lambda}\bar{m}(\lambda) & \sum_{\lambda}\tilde{P}_{3,\lambda}\bar{l}(\lambda) & \sum_{\lambda}\tilde{P}_{3,\lambda}\bar{r}(\lambda) \\ \sum_{\lambda}\tilde{P}_{4,\lambda}\bar{s}(\lambda) & \sum_{\lambda}\tilde{P}_{4,\lambda}\bar{m}(\lambda) & \sum_{\lambda}\tilde{P}_{4,\lambda}\bar{l}(\lambda) & \sum_{\lambda}\tilde{P}_{4,\lambda}\bar{r}(\lambda) \end{bmatrix} \quad (5)$$

To display a light for a specific photoreceptor excitation, the unique scaling coefficient for each LED can be found; i. e. $\alpha=\beta A^{-1}$. With this principle, to modulate rod excitations in a square-wave, for instance, with a contrast of *C* and steady cone excitation, background photoreceptor excitations are β_0=[*S M L* R_0] and the peak photoreceptor excitation is β_1 = [*S M L* R_1], where $(R_1\text{-}R_0)/R_0 = C$. First, calculate $\alpha_0 = \beta_0 A^{-1}$, and $\alpha_1 = \beta_1 A^{-1}$, then present α_0 and α_1 in a temporal order defined by a square-wave form. In doing so, rod excitations can be modulated while keeping the S-, M-, and L- cone excitations constant. Similarly, the stimulation of one cone type (S, M or L cones) can be modulated while keeping the excitations of the remaining photoreceptor types constant. One can also modulate the excitations of two or three photoreceptor types, such as modulating L cone and rod excitations while keeping M and S cone excitations constant. For cone stimuli, stimulation of one type of cone, or the combination of cone types [such as luminance at a constant chromaticity, (L+M)], can be achieved. Figure 3 describes how changes in rod excitation can be accomplished while maintaining constant cone excitations.

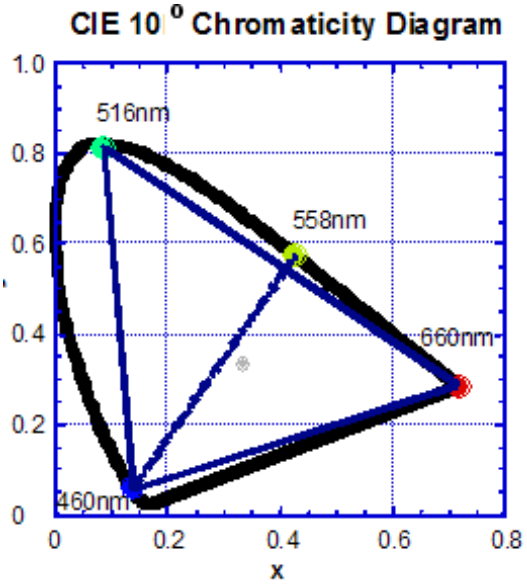

Figure 3. Achieving rod isolation with four primaries. The chromaticities of the four primaries (460, 516, 558 and 660 nm) are shown in the CIE 10° chromaticity diagram. The gray dot represents the chromaticity for a light metameric to an equal-energy-spectrum light (EES). In color matching, the EES chromaticity can be matched by a combination of three primaries (460, 516 and 660 nm). The same chromaticity can be matched by another set of primaries (460, 558 and 660 nm). When the two sets of primaries match the same chromaticity, they produce the same cone excitations. Note the two sets of primaries differ in one primary, with the rods being more sensitive to the 516 nm light than to the 558 nm light. Varying the proportion of the two matches over time produces rod modulation while maintaining a constant cone chromaticity.

4.2. Design of the four-primary photostimulator

For the two-channel four-primary photostimulator (Pokorny *et al.*, 2004), one channel is used to produce a central field and the second channel illuminates a surround. The center and surround are created with the combination of four primary channels, with light from four light emitting diodes (LEDs) combined by the use of a fiber optic assembly. Four fiber optic bundles are merged into a single bundle with the output

fed into an integrating bar spatial homogenizer terminated by a diffuser. Spectral composition is controlled by the LED spectra and interference filters sandwiched between each LED and the fiber optic bundle. The primary wavelengths for both center and surround are 460 nm, 516 nm, 558 nm and 660 nm, all with half-bandwidths of about 10 nm. Two camera lenses collimate light from the diffusers, one for the center and one for the surround. A photometric cube with a mirrored ellipse on the hypotenuse forms the center-surround field configuration. A field lens places images of the diffusers in the plane of an artificial pupil for Maxwellian view. Figure 4 shows the optical setup (left panel) and a picture (right panel) of the four-primary photostimulator.

The radiances of the primaries are controlled by an eight-channel analog output Dolby soundcard (M-Audio-Revolution 7.1 PCI). The desired output waveform is programmed as an amplitude modulation of a 20 kHz carrier. The soundcard has a 24-bit digital-to-analog converter (*DAC*) operating at a sampling rate of 192 kHz. The output of the DAC is demodulated (Puts *et al.*, 2005) and sent to voltage-to-frequency converters that provide 1 μs pulses at frequencies up to 250 kHz to control the LEDs (Swanson *et al.*, 1987). In addition to precise control of the photoreceptor excitations, the four-primary photostimulator has precise temporal stimulus control.

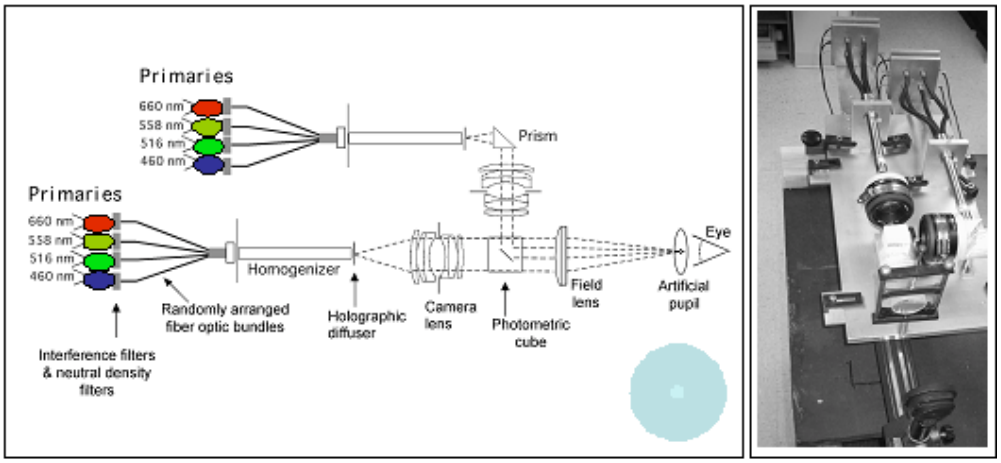

Figure 4. The optical setup and a picture of the four primary photostimulator.

4.3. Advantages of the four-primary photostimulator

Compared with traditional methodologies, the four-primary photostimulator offers several advantages. First is its capability of modulating one type of photoreceptor while keeping the excitation of the other three constant. Therefore, the four-primary photostimulator allows changes in rod or cone stimulation while maintaining the same adaptational cone chromaticity and luminance level, a critical requirement for the study of mesopic vision. Second, it can simultaneously control rod and postreceptoral signals, allowing assessment of the contributions of rods to postreceptoral luminance or chromatic processing. Third, it allows direct measurements of rod and cone functions instead of inferred from the comparison of measurements during the cone-plateau and 30-min in the dark, or inferred from the comparison of measurements between fovea and parafovea. Finally, calibration procedures have been defined that allow compensation for observer prereceptoral filtering and the small receptoral spectral sensitivity differences encountered among color-normal observers. These observer calibrations are designed to ensure that good receptor isolation can be achieved for each observer despite observer differences.

5. FOUR-PRIMARY COLORIMETRY: METHOD FOR INDEPENDENTLY STIMULATING RODS AND CONES AT A COMMON ADAPTATION LEVEL

Over the past 15 years, we have investigated mesopic vision using the four-primary photostimulator, covering color perception (Sun *et al.*, 2001a; Cao *et al.*, 2005; Cao *et al.*, 2008a), chromatic discrimination (Cao *et al.*, 2008b), and temporal processing (Sun *et al.*, 2001b; Cao

et al., 2006, 2007; Zele *et al.*, 2007, 2008; Cao & Pokorny, 2010). Here we provide two examples related to mesopic temporal processing, the first is rod suppression of cone flicker detection and the second is mesopic rod and cone reaction time. These examples use the impulse response function of the rod and cone system as a tool to help in analyzing mesopic temporal processing.

5.1. Rod-cone interactions in temporal vision

Figure 5 shows a comparison of dark adaptation function for single pulses of light (Bartlett, 1965) and light modulated at 20 Hz (Goldberg *et al.*, 1983). As rods dark-adapt, cone thresholds for pulsed lights asymptote (red line, Fig. 5), but modulated light thresholds at 20 Hz increase (green line, Fig. 5). We have performed two sets of experiments to investigate this phenomenon. The first looks at which receptoral and postreceptoral mechanisms exhibit the suppression of cone sensitivity. The second set of experiments asks whether the suppression is idiosyncratic to temporally modulated light or whether it is a general loss of temporal resolution.

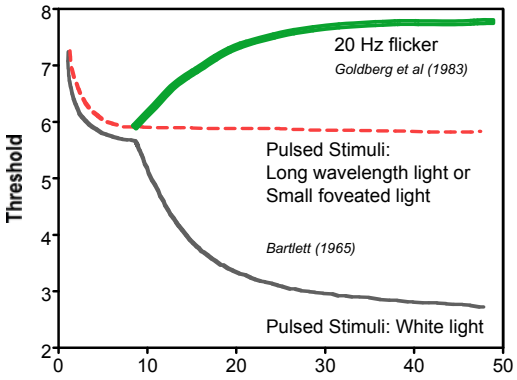

Figure 5. Detection threshold to the pulsed or modulated stimuli in the dark.

We measured critical fusion frequencies (*CFF*) for receptoral L-, M-, S- cone and postreceptoral luminance ([L+M], and [L+M+Rod]) and chromatic, [L/(L+M)] stimuli in the presence of different levels of surrounding rod activity (Cao et al., 2006). The stimulus field was 2° in diameter, positioned within a 13° surround, and centered at 7.5° in the temporal retina. The receptoral or postreceptoral excitation was modulated sinusoidally around a mean retinal illuminance of 80 Td. The surround was set to a steady retinal illuminance of 0, 0.05, 0.5, 5, 20 or 80 Td. Measurements were made either with adaptation to the stimulus field after dark adaptation (DA), or during a brief period following light adaptation (LA). Figure 6 shows the measured *CFF* for various receptoral and postreceptoral stimuli under dark adaptation condition (DA, Fig. 6A) or light adaptation condition (LA, Fig. 6B) from one observer, with the lateral suppressive rod-cone interaction occurring at low surround illuminances ≤0.5 Td. The results show that dark-adapted rods maximally suppressed the *CFF* by ~6 Hz for L-cone, M-cone, and luminance modulations (Fig. 6C). Dark-adapted rods however, showed no statistically significant suppression of S-cone CFF and only a small suppression of [L-M] *CFF* (not shown). Thus the largest suppression was found for stimuli that included a luminance component, and we infer that the lateral suppressive rod-cone interaction in cone-mediated flicker detection is strong in the MC-pathway.

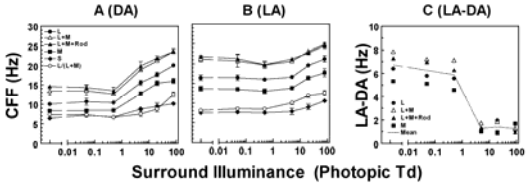

Figure 6. CFF measurements following the dark and light adaptations and the difference in CFF between with the dark and light adaptation conditions for observer DC. Left: the CFF for DA; Middle: the CFF for LA; Right: the difference in the CFF measured between LA and DA (Cao, Zele & Pokorny, 2006).

The second series of studies was designed to test whether lateral suppressive rod–cone interactions are stimulus specific, that is, only occur with the use of temporally periodic stimuli, or if the suppression is a more general visual phenomenon that can also alter cone sensitivity to double pulsed stimuli. To test this proposal, cone pathway contrast sensitivity was measured using periodic and double pulsed stimuli under viewing conditions that altered the level of rod activity in the area surrounding the stimulus (Zele et al., 2008). The stimuli (2° center/13° surround, 80 Td) were similar to CFF measurements except only the cone luminance modulation (L+M) was used. Cone temporal contrast sensitivity functions were measured for frequencies between 3-26 Hz, using a double yes-no random staircase procedure. Two-pulse discrimination (Ikeda, 1986; Burr & Morrone, 1993) was measured with a pair of 4 ms rectangular pulses displayed successively at

stimulus onset asynchronies (SOA, the time delay between two pulses) varying between 14 to 270 ms. Measurement conditions included two incremental pulses or an incremental and a decremental pulse. Cone pathway impulse response functions were derived from the periodic and pulsed data using two independent techniques. For the temporal contrast sensitivity data, the IRFs were derived using a Kramers-Krönig relation to reconstruct the temporal phase spectrum with a minimum phase assumption (Stork & Falk, 1987). Scaling and extrapolations at the low and high frequencies were conducted according to procedures described by Swanson et al., (1987). For the two-pulse summation data, we estimated the IRF using the exponentially damped, frequency modulated sinusoid model without assuming a minimum phase (Burr & Morrone, 1993). The results showed that after dark adaptation, temporal contrast sensitivity was attenuated at frequencies greater than 6–8 Hz, two-pulse contrast sensitivity decreased and the timing was altered. The mathematically derived IRFs demonstrate that after dark adaptation, the cone pathway IRF amplitude decreased and the time-to-peak was delayed. Thus dark-adapted rods altered the amplitude and timing of cone pathway temporal impulse response functions (Figure 7 for Observer *DC*).

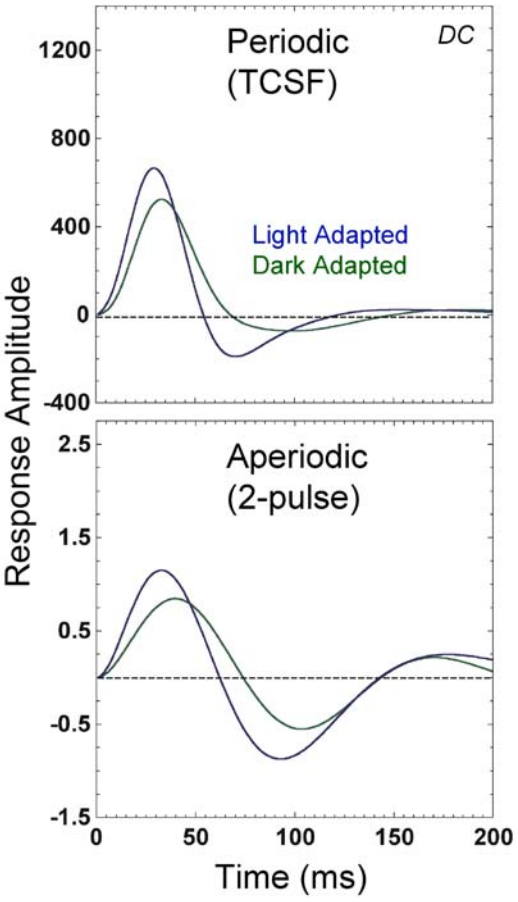

Figure 7. The derived IRFs from TCSF (top) and two-pulse summation function (bottom) under light adapted (dark lines) or dark adapted (green lines) condition (Zele, Cao & Pokorny, 2008).

5.2. Rod and cone reaction times

We measured simple reaction times for rod or cone incremental and decremental stimuli at retinal illuminance levels varying from scotopic to photopic (Cao et al., 2007). The mean reaction times decreased with higher contrast and retinal illumiance level for isolated rod (Figure 8) and isolated cone (Figure 9) stimuli. At mesopic light levels (2 and 20 Td), rod and cone reaction times were comparable at 2 Td but cone reaction times were shorter than rod reaction times (Figure 10).

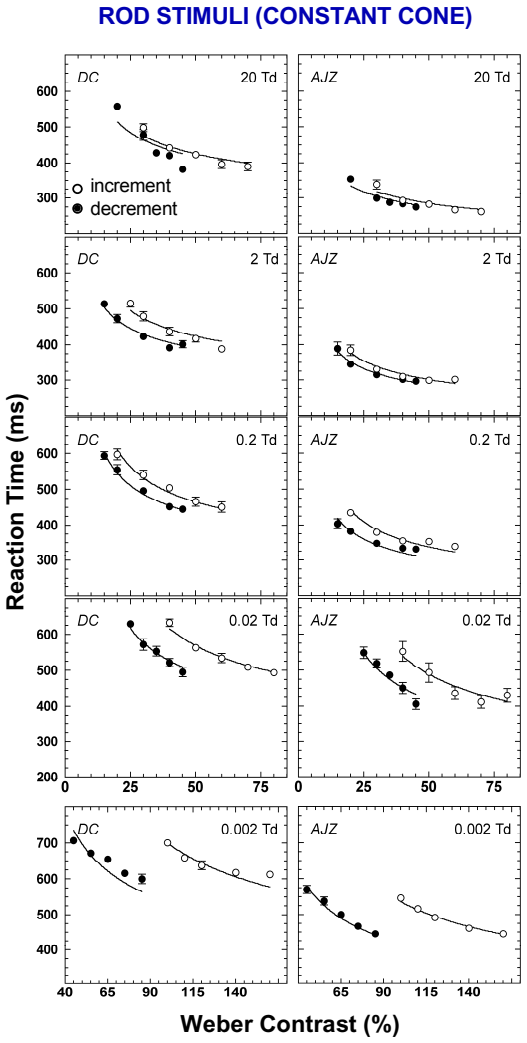

Figure 8. Reaction times to isolated rod stimuli (open circles: rod increment; solid circles: rod decrement). Data from Cao, Zele & Pokorny 2007.

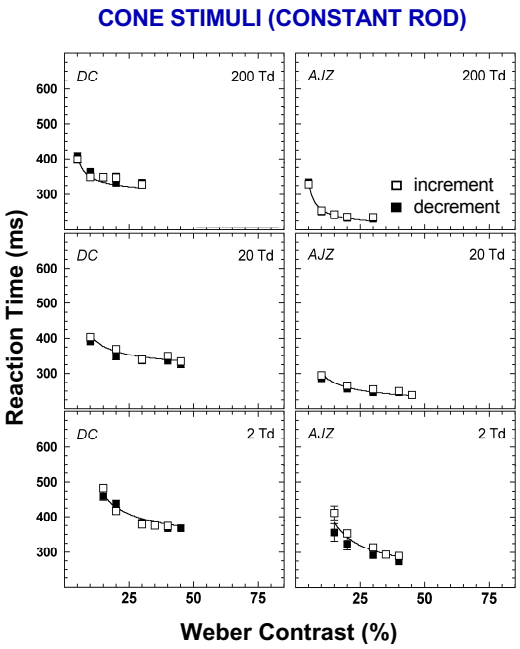

Figure 9. Reaction times to isolated cone stimuli (open squares: cone increment; solid squares: cone decrement). Data from Cao, Zele & Pokorny, 2007.

We fitted the data with a model incorporating rod and cone impulse response functions and an accumulation process that triggers a motor response (Cao et al., 2007). The sensory processing model used prototypical rod and cone temporal impulse response functions for the different light levels (Figure 11). These functions were derived from published psychophysical temporal contrast sensitivity functions and two-pulse summation data and thus included post-retinal temporal filtering. The rod or cone stimulus at each contrast and light level was convolved with the corresponding temporal impulse response function.

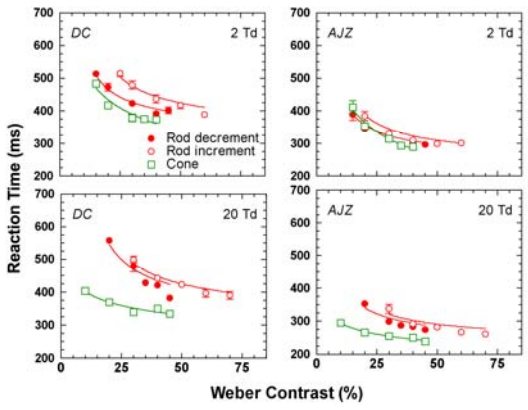

Figure 10. Reaction times to rod and cone stimuli at 2 and 20 Td (red open circles: rod increment; red solid circles: rod decrement; green open squares: cone increment). Data from Cao, Zele & Pokorny, 2007.

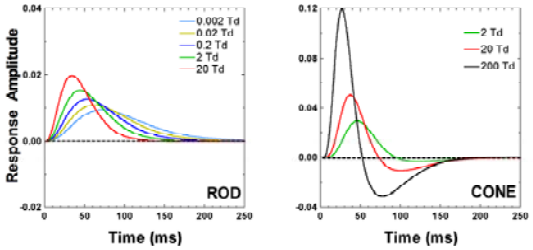

Figure 11. Estimated rod and cone impulse response functions for the retinal illuminance levels from temporal contrast sensitivity data or two-pulse summation data (Cao, Zele & Pokorny, 2007).

The model assumed the motor response was initiated when the integrated response reached a criterion value. This model fitted the data well (solid lines in Figs. 8-10) and found that an irreducible minimum reaction time for the rod stimuli were ~20ms longer than that for the cone stimuli, consistent with physiological measurements. This model provided a computational framework to describe the variation in reaction time with light level, stimulus contrast, stimulus polarity, and receptor class modulated.

6. DISCUSSION

A point we emphasize is that in mesopic vision, rod and cone signals are largely interchangeable in terms of postreceptoral visual processing. Evidence from physiology and psychophysics indicates that in photopic vision the MC-pathway is predominant in the mediation of thresholds for flicker (Schiller *et al.*, 1990), motion (Merigan *et al.*, 1991; Chapman *et al.*, 2004), object localization (Laycock *et al.*, 2007) and detection of changes in contrast (Pokorny & Smith, 1997). We may infer that these functions would be largely MC-pathway mediated at mesopic light levels.

From anatomy and physiology we know that rods and cones share common pathways. The principal rod pathway at mesopic light levels is via gap junctions between rod and cone photoreceptors. Gap junctions allow for electrical communication between cells. Physiological recordings of rod and cone photoreceptor impulse response functions are similar, showing a difference in the time to peak response on the order of 12–20 ms (Schneeweis & Schnapf, 1999; Verweij *et al.*, 1999). Primate rod and cone photovoltage responses measured directly in cones show comparable high frequency sensitivity (Hornstein *et al.*, 2005). There is some high-

pass filtering of rod signals measured in cones. For responses to stimulus change, cone signals and rod signals conveyed by gap junctions can be similar.

Decision processing for detection or action is cortically mediated, and a reasonable assumption is that decision processing uses the same rules no matter what type of photoreceptors initiate early visual processing (Cao & Pokorny, 2010). Once information leaves the retina, rod and cone initiated events should be processed in the same manner in the central nervous system. Thus at mesopic light levels near threshold temporal and spatial function should be comparable, whether vision begins with rod or cone activation. The temporal properties are similar, as described in the experiments reported here; for spatial vision, the dimensions of the cone driven receptive fields should determine common spatial properties for cone or rod input. This analysis does not take into account rod-cone interactions that may occur in the distal retina. The experiments we describe on dark-adapted rod suppression of cone temporal function were done relatively close to the fovea, at an eccentricity of 7.5°. Under these conditions, our results show that dark-adapted rods suppress cone temporal vision by 50%. The same degree of suppression occurs for directly viewed foveal stimuli (Coletta & Adams, 1984). The suppression in the peripheral retina is much greater, on the order of 90% (Alexander & Fishman, 1986). Thus using illuminants that effectively stimulate rods can dramatically improve cone function.

The reaction time data show that at mesopic levels, responses to rod and cone excitation can be similar. Again, these data were obtained at a retinal location near the fovea. At greater eccentricities, where rod density is higher and cone density lower, impulse response amplitude would be higher and reaction times for rods would be expected to be faster that for cones.

What insights may be gained from the analysis of impulse response functions? Different tasks can use input information in different ways. For example, our modelling of the reaction time data is based upon the idea that the initial rising portion of the impulse response function is a principal determinant of reaction time. However temporal order judgments, another measure of perceptual latency, yield a different dependence on field luminance. With reduction in luminance, reaction time shows a considerable change in latency whereas temporal order judgments exhibit far less dependency (Roufs, 1974; Jaskowski, 1992). This is not likely due to a change in the motor component of reaction time (Miller & Low, 2001). It is plausible to assume that reaction time is dependent on the initial portion of the internal stimulus representation whereas temporal order is dependent on the peak (Sternberg & Knoll, 1973) or temporal centroid (Williams & Lit, 1983) of the representation. Another example of performance tasks using different aspects of cortical input information can be seen in discrepancies between reaction times and the exposure durations required for detection of sinusoidal gratings with variation in grating contrast (Ejima & Ohtani, 1987). Aside from stimulus detection, stimulus strength affects the accumulation of sensory evidence until a criterion decision threshold is reached. At near-threshold stimulus contrasts, speeded responses are slower and accuracy is lower (e.g. Luce, 1986). What governs detection threshold sensitivity? One would expect the visual system to integrate over the internal stimulus representation, using all available information to decide if a stimulus is present or not.

How can we reconcile the improvement in sensitivity with dark adaptation in the case of single pulses of light with the loss of sensitivity for temporally modulated light? With dark adaptation, the amplitude of the impulse response function decreases, but this is accompanied by a longer integration time. The integrated area of the impulse response function does not change in a dramatic way. For the temporally modulated stimuli, analysis involves convolving the impulse response function with the temporal waveform of the modulated light. Detection of the modulation would occur when the modulation of the convoluted function reaches some criterion amplitude. Thus with rod dark-adaptation having the effect of lowering the amplitude and increasing the integration time, the modulated stimulus would have to be either increased in contrast or decreased in temporal frequency to reach the criterion.

The message here is: From a basic science perspective, to optimize visual function at mesopic light levels, get rods involved!

REFERENCES

Adrian W (1998). The influence of spectral power distribution for equal visual performance in roadway lighting level. *Proceedings of the Fourth International Vision at Low Light Levels Symposium, Orlando, FL: EPRI*.

Alexander KR, Fishman GA (1986). Rod influence on cone flicker detection: variation with retinal eccentricity. *Vision Research,* **26**, 827-834.

Bartlett NR (1965). Dark adaptation and light adaptation. *Vision and Visual Perception*. Graham, CH ed., 185-207. John Wiley & Sons, New York.

Burr DC, Morrone MC (1993). Impulse-Response Functions for Chromatic and Achromatic Stimuli. *Journal of the Optical Society of America a-Optics Image Science and Vision,* **10,** 1706-1713.

Cao D, Pokorny J. (2010). Rod and cone contrast gains derived from reaction time distribution modeling. *Journal of Vision,* **10** (11): 1-15.

Cao D, Pokorny J, Smith VC (2005). Matching rod percepts with cone stimuli. *Vision Research,* **45**, 2119-2128.

Cao D, Pokorny J, Smith VC, Zele AJ (2008a). Rod contributions to color perception: Linear with rod contrast. *Vision Research,* **48**, 2586-2592.

Cao D, Zele AJ, Pokorny J (2006). Dark-adapted rod suppression of cone flicker detection: Evaluation of receptoral and postreceptoral interactions. *Visual Neuroscience,* **23**, 531-537.

Cao D, Zele AJ, Pokorny J (2007). Linking impulse response functions to reaction time: Rod and cone reaction time data and a computational model. *Vision Research,* **47**, 1060-1074.

Cao D, Zele AJ, Pokorny J (2008b). Chromatic discrimination in the presence of incremental and decremental rod pedestals. *Visual Neuroscience*, 399-404.

Chapman C, Hoag R, Giaschi D (2004). The effect of disrupting the human magnocellular pathway on global motion perception. *Vision Research,* **44**, 2551-2557.

Coletta NJ, Adams AJ (1984). Rod-cone interaction in flicker detection. *Vision Research,* **24**, 1333-1340.

Conner JD (1982). The temporal properties of rod vision. *Journal of Physiology,* **332**, 139-155.

Crawford BH, Palmer DA (1985). The scotopic visibility curve and cone intrusion. *Vision Research,* **25**, 863-866.

Crook JD, Davenport CM, Peterson BB, Packer O, Detwiler PB, Dacey DM (2009). Parallel ON and OFF cone bipolar inputs establish spatially coextensive receptive field structure of blue-yellow ganglion cells in primate retina. *Journal of Neuroscience,* **29**, 8372-8387.

Dacey DM (2000). Parallel pathways for spectral coding in primate retina. *Annual Review of Neuroscience;* **23**, 743-775.

Dacey DM, Lee BB (1994). The 'blue-on' opponent pathway in primate retina originates from a distinct bistratified ganglion cell type. *Nature,* **367**, 731-735.

Daw NW, Jensen EJ, Bunken WJ (1990). Rod pathways in the mammalian retinae. *Trends in Neurosciences,* **13,** 110-115.

Derrington, AM, Krauskopf J, Lennie P (1984). Chromatic mechanisms in lateral geniculate nucleus of macaque. *Journal of Physiology (London),* **357**, 241-265.

Ejima Y, Ohtani Y (1987). Simple reaction time to sinusoidal grating and perceptual integration time: Contributions of perceptual and response processes. *Vision Research,* **27**, 269-276.

Estévez O, Spekreijse H (1982). The "silent substitution" method in visual research. *Vision Research,* **22**, 681-691.

Field GD, Greschner M, Gauthier JL, Rangel C, Shlens J, Sher A, Marshak DW, Litke A M, Chichilnisky EJ (2009). High-sensitivity rod photoreceptor input to the blue-yellow color opponent pathway in macaque retina. *Nature Neuroscience,* **12**, 1159-1164.

Frumkes TE, Naarendorp F, Goldberg SH, (1986). The influence of cone adaptation upon rod mediated flicker. *Vision Research,* **26**, 1167-1176.

Goldberg SH, Frumkes TE, Nygaard RW (1983). Inhibitory influence of unstimulated rods in the human retina: evidence provided by examining cone flicker. *Science,* **221**, 180-182.

Gouras P, Link K (1966). Rod and cone interaction in dark-adapted monkey ganglion cells. *Journal of Physiology,* **184**, 499-510.

He, Y, Rea MS, Bierman A, Bullough JD

(1997). Evaluating light source efficacy under mesopic conditions using reaction times. *Journal of the Illuminating Engineering Society,* **28**, 125-138.

Hornstein EP, Verweij J, Li PH, Schnapf JL (2005). Gap-junctional coupling and absolute sensitivity of photoreceptors in Macaque retina. *Journal of Neuroscience,* **25,** 11201-11209.

Ikeda M (1986). Temporal impulse response. *Vision Research,* **26**, 1431-1440.

Jaskowski P (1992). Temporal-order judgment and reaction time for short and long stimuli. *Psychological Research,* **54**, 141-145.

Laycock R, Crewther SG, Crewther DP (2007). A role for the 'magnocellular advantage' in visual impairments in neurodevelopmental and psychiatric disorders. *Neuroscience and Biobehavioral Reviews,* **31**, 363-376.

Lee BB (1996). Receptive field structure in the primate retina. *Vision Research,* **36,** 631-644.

Lee BB, Pokorny J, Smith VC, Martin PR, Valberg A (1990). Luminance and chromatic modulation sensitivity of macaque ganglion cells and human observers. *Journal of the Optical Society of America A,* **7**, 2223-2236.

Lee BB, Smith VC, Pokorny J, Kremers J (1997). Rod inputs to macaque ganglion cells. *Vision Research,* **37**, 2813-2828.

Lewis AL (1999). Visual performance as a function of spectral power distribution of light sources at luminances used for general outdoor lighting [with discussion]. *Journal of the Illuminating Engineering Society,* **28**, 37-42.

Luce RD (1986). Response Times: Their Role in Inferring Elementary Mental Organization. *Oxford University Press, New York*.

Merigan WH, Byrne CE, Maunsell JH (1991). Does primate motion perception depend on the magnocellular pathway? *Journal of Neuroscience,* **11**, 3422-3429.

Miller JO, Low K (2001). Motor processes in simple, go/no-go, and choice reaction time tasks: a psychophysiological analysis. *Journal of Experimental Psychology: Human Perception and Performance,* **27**, 266-289.

Pokorny J, Smith VC (1997). Psychophysical signatures associated with magnocellular and parvocellular pathway contrast gain. *Journal of the Optical Society of America A,* **14**, 2477-2486.

Pokorny J, Smith VC (2004). Chromatic Discrimination. In *The Visual Neuroscience*, vol. 2. Chalupa LM. & Werner JS eds., 908-923. MIT Press, Cambridge, MA.

Pokorny J, Smithson H, Quinlan J (2004). Photostimulator allowing independent control of rods and the three cone types. *Visual Neuroscience,* **21**, 263-267.

Purpura K, Kaplan E, Shapley RM (1988). Background light and the contrast gain of primate P and M retinal ganglion cells. *Proceedings of the National Academy of Sciences of the United States of America,* **85**, 4534-4537.

Puts MJH, Pokorny J, Quinlan J, Glennie L (2005). Audiophile hardware in vision science; the soundcard as a digital to analog converter. *Journal of Neuroscience Methods,* **142**, 77-81.

Rea MS, Bierman A, McGowan T, Dickey F, Havard J (1997). A field test comparing the effectiveness of metal halide and high pressure sodium illuminats under mesopic conditions. *Proceedings of the NPL-CIE-UK Conference, Visual Scales: Photometric and Colorimetric Aspects. Teddington, UK: NPL***,** 60-64.

Roufs JA (1974). Dynamic properties of vision. V. Perception lag and reaction time in relation to flicker and flash thresholds. *Vision Research,* **14**, 853-869.

Schiller PH, Logothetis NK, Charles ER (1990). Role of the color-opponent and broad-band channels in vision. *Visual Neuroscience,* **5**, 321-346.

Schneeweis DM, Schnapf JL (1999). The photovoltage of macaque cone photoreceptors: adaptation, noise, and kinetics. *J Neurosci,* **19**, 1203-1216.

Shapiro AG, Pokorny J, Smith VC (1996). Cone-rod receptor spaces, with illustrations that use CRT phosphor and light-emitting-diode spectra. *Journal of the Optical Society of America A,* **13**, 2319-2328.

Sharpe LT, Stockman A (1999). Rod pathways: The importance of seeing nothing. *Trends in Neurosciences,* **22**, 497-504.

Smith VC, Pokorny J (1975). Spectral sensitivity of the foveal cone photopigments between 400 and 500 nm. *Vision Research,* **15**, 161-171.

Stabell U, Stabell B (1999). Rod-cone color mixture: effect of size and exposure time. *Journal of the Optical Society of America A,* **16**, 2638-2642.

Sternberg S, Knoll RL (1973). The perception of temporal order: Fundamental issues and a general method. In *Attention and performance*, vol. IV. Kornblum S ed., 629-685. Academic Press, New York.

Stork DG, Falk DS (1987). Visual temporal impulse response functions from flicker sensitivities. *Journal of the Optical Society of America A,* **4**, 1130-1135.

Sun H, Pokorny J, Smith VC (2001a). Brightness Induction from rods. *Journal of Vision,* **1**, 32-41.

Sun H, Pokorny J, Smith VC (2001b). Rod-cone interaction assessed in inferred postreceptoral pathways. *Journal of Vision,* **1**, 42-54.

Swanson WH, Ueno T, Smith VC, Pokorny J (1987). Temporal modulation sensitivity and pulse detection thresholds for chromatic and luminance perturbations. *Journal of the Optical Society of America A,* **4**, 1992-2005.

Thomas LP, Buck SL (2006). Foveal and extra-foveal influences on rod hue biases. *Visual Neuroscience,* **23**, 539-542.

Verweij J, Peterson BB, Dacey DM, Buck SL (1999). Sensitivity and dynamics of rod signals in H1 horizontal cells of the macaque monkey retina. *Vision Research,* **39**, 3662-3672.

Virsu V, Lee BB (1983). Light adaptation in cells of macaque lateral geniculate nucleus and its relation to human light adaptation. *Journal of Neurophysiology,* **50**, 864-878.

Virsu V, Lee BB, Creutzfeldt OD (1987). Mesopic spectral responses and the Purkinje shift of macaque lateral geniculate cells. *Vision Research,* **27**, 191-200.

Walkey HC, Orrevetelainen P, Barbur JL, Halonen L, Goodman T, Alferdinck J, Freiding A, Szalmás A (2007). Mesopic visual efficiency II: reaction time experiments *Lighting Research and Technology,* **39**, 335-354.

Wiesel T, Hubel DH (1966). Spatial and chromatic interactions in the lateral geniculate body of the rhesus monkey. *Journal of Neurophysiology,* **29**, 1115-1156.

Williams JM, Lit A (1983). Luminance-dependent visual latency for the Hess effect, the Pulfrich effect, and simple reaction time. *Vision Research,* **23**, 171-179.

Zele AJ, Cao D, Pokorny J (2007). Threshold units: A correct metric for reaction time? *Vision Research,* **47**, 608-611.

Zele AJ, Cao D, Pokorny J (2008). Rod-cone interactions and the cone pathway temporal impulse response. *Vision Research,* **48**, 2593-2598.

ACKNOWLEDGEMENTS

Our studies have been supported by National Eye Institute grant EY00901. We thank Jules Quinlan for technical assistance with the optical system and Linda Glennie for technical assistance in computer programming. We also thank our long time collaborators, Vivianne Smith, Hao Sun, Barry Lee, Andrew Zele, Hannah Smithson, and Arthur Shapiro.

AUTHORS

Joel Pokorny
Visual Science Laboratories
The University of Chicago
940 East 57th Street
Chicago, IL 60637, USA
Tel. +1 773 702-1983
Fax 1 773 702-0939
j-pokorny@uchicago.edu

Dingcai Cao
Department of Surgery
Section of Ophthalmology and Visual Science
The University of Chicago
5841 South Maryland Avenue
MC 2114, Chicago, IL 60637, USA
Tel. +1 773 834-5978
Fax +1 773 834-5970
d-cao@uchicago.edu